Marine Biology 86, 283–295 (1985)

Marine Biology
International Journal on Life in Oceans and Coastal Waters

Propulsion efficiency and cost of transport for copepods: a hydromechanical model of crustacean swimming

M. J. Morris, G. Gust and J. J. Torres

University of South Florida, Department of Marine Science; St. Petersburg, Florida 33701, USA

Abstract

In the absence of direct measurement, costs of locomotion to small swimming Crustacea (< 10 mm) have been derived exclusively through application of the fluid dynamic theory. Results indicate very low swimming costs, and contradict experimental data on larger Crustacea (15 to 100 mm) that suggest a three-fold increase in metabolic rate with increasing swimming speed. This paper introduces a swimming model that analyzes the hydrodynamic forces acting on a crustacean swimming at non-steady velocity. The model treats separately the hydrodynamic forces acting on the body and the swimming appendages, approximating the simultaneous solution of equations quantifying the drag and added-mass forces on each by stepwise integration. Input to the model is a time-series of instantaneous swimming-appendage velocities. The model output predicts a corresponding time-series of body velocities as well as the mechanical energy required to move the swimming appendages, dissipated kinetic energy, and metabolic cost of swimming. Swimming of the calanoid copepod *Pleuromamma xiphias* (Calanoida) was analyzed by extrapolating model parameters from data available in the literature. The model predictions agree well with empirical observations reported for larger crustaceans, in that swimming for copepods is relatively costly. The ratio of active to standard metabolism for *P. xiphias* was > 3. Net cost of transport was intermediate to the values found experimentally for fish and larger crustaceans. This was a consequence of the predicted mechanical efficiency (34%) of the copepod's paddle propulsion, and of increased parasitic resistance resulting from non-steady velocity swimming.

Introduction

A substantive fraction of the energy transferred at the phytoplankton-herbivore interface in the world's oceans is dissipated in the swimming metabolism of small (< 10 mm) crustacean zooplankton. Several studies have attempted to quantify the cost of swimming in small Crustacea (Vlymen, 1970; Klyashtorin and Yarzhombek, 1973; Svetlichnyi *et al.*, 1977), but the technical difficulty of collecting data on energy consumption vs swimming speed of a very small, intermittently swimming crustacean has precluded any direct measurements. Instead, costs of locomotion have been calculated using simplified principles of fluid dynamics. Results obtained using the hydrodynamic theory suggest that swimming costs for small Crustacea range from negligible (Vlymen, 1970) to at most 1.25 times the standard (basal) metabolic rate (Klyashtorin and Yarzhombek, 1973; Svetlichnyi *et al.*, 1977). In contrast, empirically determined swimming costs in larger (15 to 100 mm) crustacean zooplankton suggest that increased swimming speed results in an energy consumption of three to five times that typical of standard metabolism (Ivlev, 1963; Halcrow and Boyd, 1967; Quetin *et al.*, 1978; Torres *et al.*, 1982; Torres and Childress, 1983). The schism between theoretically and empirically derived swimming costs remains unexplained, but the disparity between the two is too large to be due solely to size differences in the crustaceans considered by each type of treatment (Torres, 1984).

The calculations of crustacean swimming costs by Vlymen (1970) were based on the dissipation of energy through body drag and were formulated without consideration of the propulsive process. Three factors not considered in the swimming cost analyses were: (1) energy losses during swimming-appendage recovery strokes, (2) hydrodynamic added-mass effects due to swimming-appendage acceleration, and (3) increased parasite resistance resulting from intermittent non-steady velocity swimming.

Blake analyzed paddle propulsion in angelfish swimming at steady velocity (Blake, 1979, 1980). He used a blade-element technique to calculate the hydrodynamic forces acting on a rotating pectoral fin, and quantified the

energy losses due to recovery strokes and fin accelerations (Factors 1 and 2 above).

In this paper we expand on Blake's work by modeling the non-steady velocity swimming of crustaceans (Factors 1, 2, and 3 above). Our method uses a coordinated stepwise summation of forces acting on both the body and the various propulsive elements of a swimming crustacean over small time and distance increments. The technique approximates a simultaneous integration of the equations describing the hydrodynamic forces acting on the body and swimming appendages. The model input is a time series of angular velocities for each appendage, from which a time series of body velocities is predicted (all of which can be obtained from high-speed motion pictures). In addition, the model quantifies the kinetic energy dissipated in the fluid, the mechanical energy required to move the appendages, and the metabolic cost of swimming. An analysis of swimming in the copepod *Pleuromamma xiphias* (Calanoida) indicates that much of the gap between the theoretical and empirical results reported in the literature can be eliminated using our model.

Swimming model

Our model is of general applicability to a variety of swimming mechanisms used by crustaceans, and requires only that the propulsion be based on the resistance of moving appendages. The propulsion (thrust) of each appendage and body effects (parasitic resistance) are treated as decoupled processes. That is, we assume that during swimming each pleopod moves through fluid that is not significantly changed by the boundary layer developing around the animal body, or by motions of adjacent pleopods.

Thrust and parasite resistance are described by an equation of force that includes drag and the effects of hydrodynamic added-mass that arise from accelerations (Morrison *et al.*, 1950). Integration of these forces over the distance travelled by the pleopods and by the body during a complete swimming cycle yields the mechanical energy required to move the pleopods, the resulting kinetic energy of the animal, and the energy lost to the fluid. This in turn allows calculation of mechanical efficiency, and (by utilizing independently acquired values of muscular efficiency) the metabolic cost of transport. Table 1 introduces the model parameters, symbols, and definitions used in the text.

The general equation describing the in-line hydrodynamic force (F) acting on an object accelerating in a fluid is (Morrison *et al.*, 1950):

$$F = MdU/dt + \varrho K_I \hat{V} dU/dt + \tfrac{1}{2} C_d A U^2, \quad (1)$$

where M = the mass of the object, K_I = the hydrodynamic added-mass coefficient, $\hat{V}$ = a characteristic volume of the object, C_d = the drag coefficient, A = the projected area normal to the direction of motion, U = the velocity of the object relative to the fluid, ϱ = the density of the water, and t = time.

Table 1. Model parameters, symbols and definitions used in text

Symbol	Meaning (definition)
A	Area
a	Acceleration
β	Angle between swimming leg and long axis of crustacean body
C_d	Drag coefficient
D	Drag
E_{mech}	Mechanical efficiency (the ratio of work required to move an animal through water to the work expended by the swimming appendages in actually doing so [Eq. 10])
E_m	Muscle efficiency (the ratio of work expended by the swimming appendages to the chemical energy expended by the muscular/nervous system of the animal)
E_{swim}	Swimming efficiency (the ratio of work required to move an animal through water to the chemical energy expended by the muscular/nervous system of the animal: $E_{swim} = E_{mech} \times E_m$)
F	Force
K_I	Hydrodynamic added-mass coefficient
M	Mass
ϱ	Density of seawater
r	Distance along swimming leg from attachment point
Re	Reynolds number
s	Distance travelled by animal
t	Time
T	Thrust
U	Velocity of fluid
U_{crit}	Maximum swimming velocity that can be maintained for 1 h
$\hat{V}$	Characteristic volume
V_B	Velocity of animal
ω	Radial velocity of swimming leg
Wk_{aer}	Total metabolic work (chemical energy used for swimming)
Wk_{in}	Mechanical work performed moving swimming leg through water
Wk_{out}	Mechanical work performed overcoming drag and accelerating the animal and its entrained fluid

The coefficients K_I and C_d are functions of the shape of the object, the Reynolds number (Re) of the flow, and for an oscillating object, the period parameter (cf. Goring and Raichlen, 1979). For an object with a characteristic length, l, Re relates the inertial to viscous fluid forces:

$$\mathrm{Re} = \varrho l U/\mu. \quad (2)$$

Eq. (1) is used to calculate the force, F_p, exerted by the fluid on a moving pleopod. The reactive force to this is the force exerted by the animal's muscles on the fluid as they move the appendage. The forward component of F_p

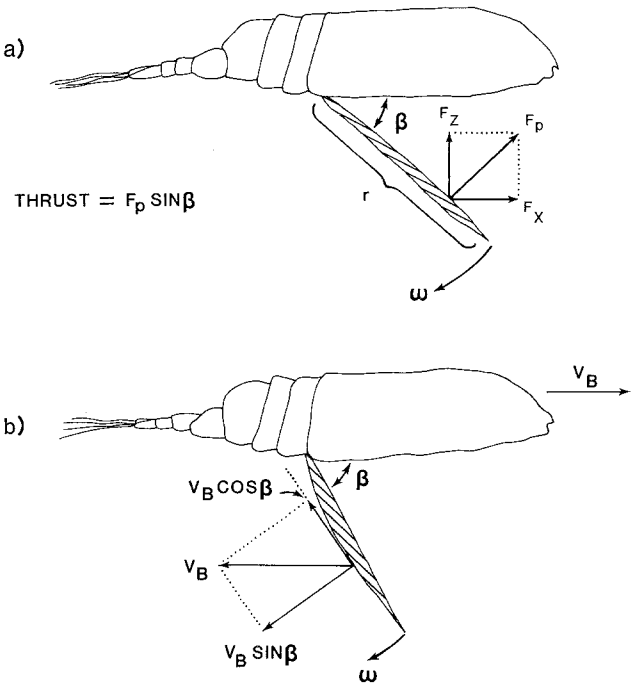

Fig. 1. *Pleuromamma xiphias.* (a) Hydrodynamic force, F_p, acting on a pereiopod pair rotating at angular velocity ω; the forward-directed component of F_p is the thrust. (b) The hydrodynamic force F_p arises from the normal component of fluid flow past the leg; this is a function of ω and the copepod body velocity, V_B [see Eq. (5)]. Drawings are schematic and not to scale

(Fig. 1 a) is the thrust (T) which depends on the angle (β) between the pleopod and body (Nachtigall, 1974):

$$T = F_p \sin\beta = F_p \sin \omega t. \tag{3}$$

Eq. (1) is also used to calculate the acceleration of the animal body which results from the thrust force.

The model operates in a two-step mode by first calculating the thrust produced by the rotation of a pleopod through a small-angle increment ($\Delta\beta$) and, from this, the resulting differential of acceleration, change in velocity, and displacement of the animal. The process is repeated over the sequence of pleopod movements in an entire swimming cycle (i.e., power and recovery strokes). To allow for the simultaneous movement of several limbs, and for non-steady velocity of these limbs, the model is synchronized to small time intervals (Δt) of constant duration. The most important model input (determined from cinematic records) is the time history of the pleopod position expressed by the relationship:

$$\beta_j = \int_{t_o}^{t_j} \omega(t)\, dt = \sum_j \Delta\beta_j, \tag{4}$$

where j represents the summation index of the time intervals.

Pleopod movement

The force acting on a rotating swimming leg is estimated by considering the local instantaneous force ΔF_{ij} on a small section of the leg at position r_i (r is the radial distance along the leg from the point of attachment) and at an angle β_j. It is assumed to depend only on the instantaneous velocity and acceleration of that section relative to the fluid (classified as resistive theory by Lighthill, 1972). Further, the force normal to the leg is considered to arise only from the normal component of flow (described as cross-flow principle by Hoerner, 1965).

The force of each section, ΔF_{ij}, is calculated from Eq. (1) with the total force, F_p, determined by subsequent summation of ΔF_{ij} over the length of the leg (note that F_p is still a function of angle position). The local velocity (U_{ij}) normal to the leg depends on the angular velocity (ω), the velocity of the animal (V_B), the angle β_j, and the radial position r_i (Blake, 1979; see also present Fig. 1 b):

$$U_{ij} = \omega r_i - V_{Bj} \sin\beta_j. \tag{5}$$

The hydrodynamic coefficients (C_d, K_I) and dimensions (M, $\hat{V}$, A) of the leg vary with radial distance as well and must be calculated at each r_i.

Body movement

The thrust (T_j) produced by movement of the pleopod through the angle increment ($\Delta\beta_j$) minus the drag [third term in Eq. (1)] will accelerate the mass and hydrodynamic added mass of the animal. To calculate the animal body acceleration (a_j), the drag and the hydrodynamic coefficients are determined by using the body velocity at the previous time interval (V_{Bj-1}). By assuming constant acceleration during the interval j, the final velocity is:

$$V_{Bj} = V_{B(j-1)} + a_j(\Delta t_j), \tag{6}$$

and the displacement (Δs) of the animal is:

$$\Delta s_j = V_{B(j-1)}\,\Delta t_j + \tfrac{1}{2}\, a_j (\Delta t_j)^2. \tag{7}$$

Energetics

The mechanical work (Wk_{in}) generated by the animal by moving its pleopod is found by integrating the product of local force (ΔF_{ij}) and distance travelled ($r_i \Delta\beta_j$) over the length of the leg (l) and the angle swept in a complete stroke from initial leg position (β_o) to final leg position (β_f) (Blake, 1979):

$$Wk_{in} = \int_{r=0}^{l} \int_{\beta_o}^{\beta_f} F(r')\, r'\, dr'\, d\beta = \sum_i \sum_j \Delta F_{ij}\, r_i\, \Delta\beta_j. \tag{8}$$

The useful work done (Wk_{out}) is the thrust times the distance travelled by the animal (from initial position s_o to final position s_f):

$$Wk_{out} = \int_{s_o}^{s_f} T\, ds = \sum_j T_j \Delta s_j, \tag{9}$$

and is integrated over the same stroke as in Eq. (8).

The mechanical efficiency of propulsion is:

$$E_{mech} = (Wk_{out})\,(Wk_{in})^{-1}, \tag{10}$$

where Wk_{out} and Wk_{in} are calculated from a complete swimming cycle (i.e., power and recovery strokes of the total set of pleopod pairs).

The total or metabolic swimming cost (Wk_{aer}) is calculated from the muscular efficiency E_m (Hill, 1950):

$$Wk_{aer}=(Wk_{in})\,(E_m)^{-1}. \quad (11)$$

The overall swimming efficiency (E_{swim}) is, therefore:

$$E_{swim}=(Wk_{out})\,(Wk_{aer})^{-1}=(E_{mech})\,(E_m). \quad (12)$$

The energy expended by the crustacean to move a unit mass a unit distance is the cost of transport, and may be expressed as either:

$$\text{Total cost of transport} = (Wk_{aer}+\text{standard respiration})\,(M\Delta s)^{-1} \quad (13)$$

or, alternatively,

$$\text{Net cost of transport} = Wk_{aer}\,(M\Delta s)^{-1}. \quad (14)$$

Application of model to copepod swimming

Although there is no complete set of input parameters for any crustacean species, sufficient data are available from a variety of species for a first test of the model. Extrapolations from published data and assumptions about parameters (described below) have been made for the swimming of the oceanic calanoid copepod *Pleuromamma xiphias* at 20 °C.

The copepod *Pleuromamma xiphias* was chosen because it is a strong diurnal vertical migrator and a powerful swimmer (Hopkins, 1982). In addition, respiration data for this species have been collected (Morris, unpublished data) and preserved specimens (adult females) were available for geometric measurement.

Our analysis addressed the hopping motion, usually associated with escape reactions, that is accomplished by the backward movement of the thoracic swimming legs (pereiopods). A cinematic study describing this mode of swimming in cyclopoid copepods has been published (Strickler, 1975), and the symmetry and single plane of movement of the pereiopods allows a simplified analysis of forces in two dimensions. Swimming of *Pleuromamma xiphias* may involve movements of other limbs, such as the first and second antennae, abdominal and furcal oscillations, or combinations of these. However, quantitative descriptions of the motions have not been reported, and cannot be analyzed.

Escape reaction

Since quantitative descriptions of leg movements of calanoids are not available, the power and recovery stroke sequence was assumed to be similar to that of the cyclopoid copepod *Cyclops* sp. Each pair of pereiopods (swimming legs) are rigidly connected to each other and act as a single unit. They are initially directed forward at an angle of about 45° to the long axis of the copepod (Fig. 2 a). The posterior legs (identified as P4) begin the power stroke sequence by swinging backward while the remaining legs stay motionless. Halfway through the P4 power stroke, the next set of legs (P3) begins to move (Fig. 2 b). The remaining legs (P2 and P1) follow in a similar pattern and the power stroke ends when P1 reaches its posterior position. Immediately, the recovery stroke begins. All four pereiopods move in unison to their anterior position. The total power stroke sequence (P4–P1) is equal in duration to the recovery stroke. Thus, each swimming leg moves 2.5 times faster during the power stroke than during the recovery stroke (based on mean angular velocity).

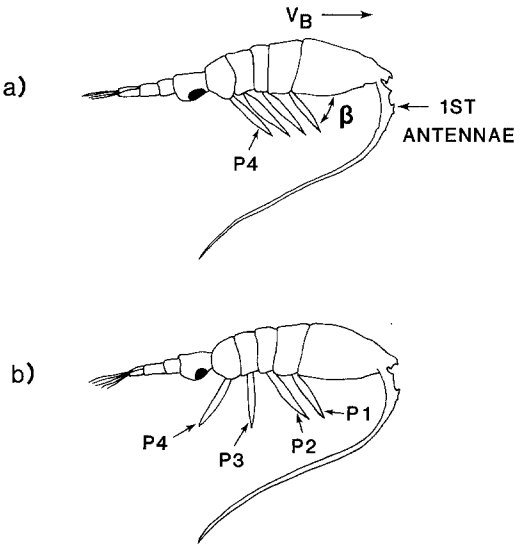

Fig. 2. *Pleuromamma xiphias.* Power-stroke sequence of escape reaction. (a) Initially, the pereiopod pairs are directed forward at an angle of 45 ° with the long axis of the body. (b) The first set of legs to move, P4, are halfway through their stroke ($\beta = 112$ °) and the next set, P3, are just beginning to move; this timing pattern continues until all four pairs of legs are at 180 °. (Drawings are schematic and not to scale)

Angular velocity of the pereiopods

The *Cyclops* sp. filmed by Strickler (1975) moved its pereiopods through 135° in 4 ms during the power stroke. The mean angular velocity was therefore 589 rad s^{-1}. *Cyclops* sp. (1.5 mm length) is smaller than *Pleuromamma xiphias* (6 mm length) and probably moves its pereiopods faster. In dytiscid water beetles, mean leg-beating frequency (f) decreased with increasing beetle length (L) through the relationship (Nachtigall, 1977):

$$f \propto L^{-0.39}. \quad (15)$$

Applying this scaling relationship to copepods (for lack of species-specific data) results in a mean angular velocity of 343 rad s^{-1} for *P. xiphias*.

In water beetles (Nachtigall, 1974) and in angelfish (Blake, 1979), the angular velocity of the paddles was greatest when they were normal to the body (i.e., $\beta = 90°$). This maximizes mechanical efficiency because muscular effort is greatest where thrust production is greatest ($\sin\beta = 1$). To simulate this pattern in the model, the angular velocity of the pereiopods was made to follow a sine function (a precise description of copepodan leg motions was not available and the sinusoidal pattern was assumed). The total duration of leg movement was divided into 50 equal time intervals of length Δt corresponding to a change of 1 in the value of a counter (the variable J in the following equations). Thus, the leg moved from its initial position β_o at time t_o, where $J=0$, to its final position β_f at t_f, where $J=50$. The position of the leg at a given value of the counter was set at:

$$\beta_j = -(3/8)\,\pi\,\{\cos[\pi J/50] - 1\} + (1/4)\,\pi, \qquad (16)$$

which satisfies the boundary conditions of: $\beta_o = 45°$ at $t=0$ ($J=0$) and $\beta_f = 180°$ at $t_f (J=50)$.
Angular velocity was therefore:

$$\omega_j = k \sin[(J/50)\,\pi]. \qquad (17)$$

The analysis was performed over a ten-fold range of arbitrarily chosen angular velocities to examine the variation of cost of transport and respiration with swimming speed. This was done by choosing values of Δt and k (amplitude of angular velocity function) corresponding to mean angular velocities ranging from 343 rad s^{-1}, the top speed predicted by the scaling argument (Eq. 15) and 34.3 rad s^{-1}. The associated values of k or maximum angular velocity were 539 to 53.9, respectively.

During the recovery stroke it was assumed that angular velocity was constant and 2.5 times lower than $\bar{\omega}$ during the power stroke.

Hydrodynamic coefficients and Reynolds numbers

The Reynolds number (Re) of the pereiopod of *Pleuromamma xiphias* varies from low values near the copepod body to 1 300 (based on an upper limit of 600 rad s^{-1} and a width of 1.5 mm) at the distal end. An empirical formula for the drag coefficient of a cylinder normal to flow (White, 1974) was used in the model, with Re based on cylinder diameter:

$$C_d = 1 + 10\,(\mathrm{Re})^{-2/3}. \qquad (18)$$

The equation is valid for $1 \leqq \mathrm{Re} \leqq 100\,000$.

The shape of the pereiopod is more complex and varies from being a flattened cylinder near the basis (pivot point) to nearly plate-like at the distal segments. Drag coefficients measured for flat plates normal to flow (Thom and Swart, 1940) are compared to those of a cylinder [calculated from Eq. (18)] in Fig. 3. At $\mathrm{Re} > 100$ there is little difference, while for $1 < \mathrm{Re} < 100$ the curves cross. Since flows with low Re occur near the pivot point where the legs are more cylindrical, White's formula was used.

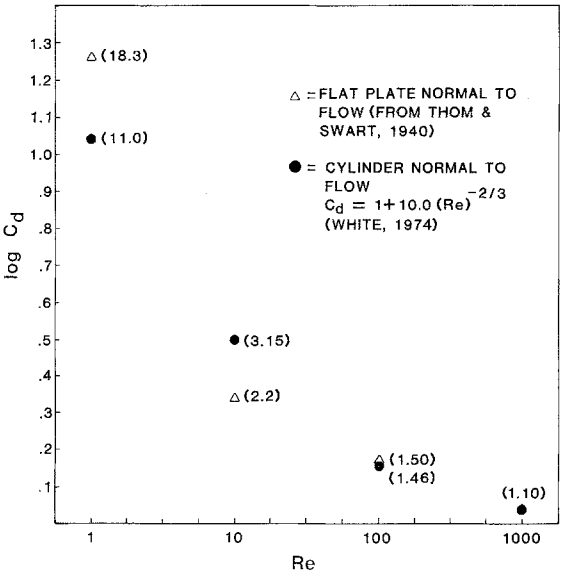

Fig. 3. Drag coefficients of flat plates and cylinders normal to steady flow at $1 \leqq \mathrm{Re} \leqq 1000$. Re is based on plate width and cylinder diameter

The hydrodynamic added-mass forces on the legs were calculated by using a value of 1.0 for K_I with the characteristic fluid volume ($\hat{V}$) equal to that of the cylinder generated by rotating the pereiopod pair about its long axis (Blake, 1979).

Both the drag and added-mass coefficients of an oscillating appendage will deviate from their values in a steady flow. The period parameter, $2\,\pi X/W$ (X = amplitude of motion, in this case one half the excursion distance of the leg during its stroke; W = the width of the leg pair), varies from 7.4 at the distal end to 6.3 at the middle of the leg. In this range, the measured average added-mass coefficient of an oscillating flat plate varied from 0.9 to 1.0 at the distal and mid points, respectively (Goring and Raichlen, 1979). Thus, our assumed value of $K_I = 1.0$ is likely to overestimate added-mass forces, but not by more than 10%. In contrast, the drag coefficient increases as the period parameter gets smaller, and to a certain extent the errors introduced by using steady-flow values will cancel.

The drag coefficient of the body (C_d) was calculated from the empirically determined equation (Vlymen, 1970) for the copepod *Labidocera trispinosa* (Re based on copepod length):

$$C_d = 85.2\,(\mathrm{Re})^{-0.8}. \qquad (19)$$

In our model, 12% of copepod mass was chosen as the mean value of added mass ($m = \varrho K_I \hat{V}$) based on the calculations for *L. trispinosa* by Vlymen (1970):

$$m = 0.12\,M. \qquad (20)$$

It should be noted that K_I values for both pereiopod and copepod body are based on theoretical flow in an inviscid fluid. Although treated as constants here, they will vary with Re and with period parameter.

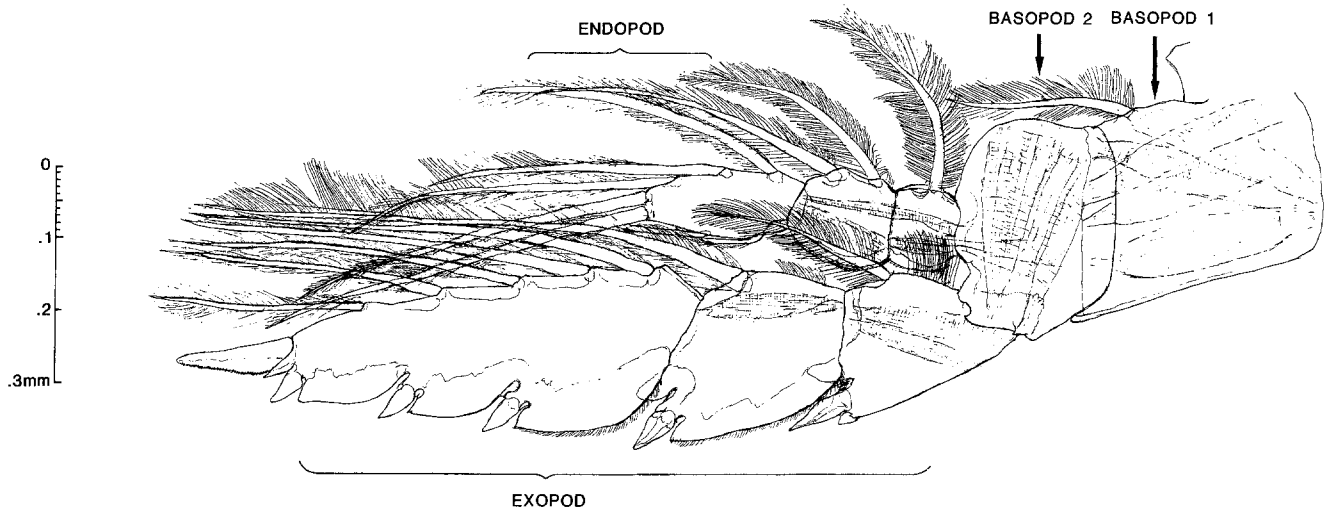

Fig. 4. *Pleuromamma xiphias.* Anterior view of left P4 (fourth pereiopod) from a camera-lucida tracing. Pereiopod pairs are rigidly attached to each other at Basopod 1 segment. During the power stroke, the pereiopod would move into the plane of the picture

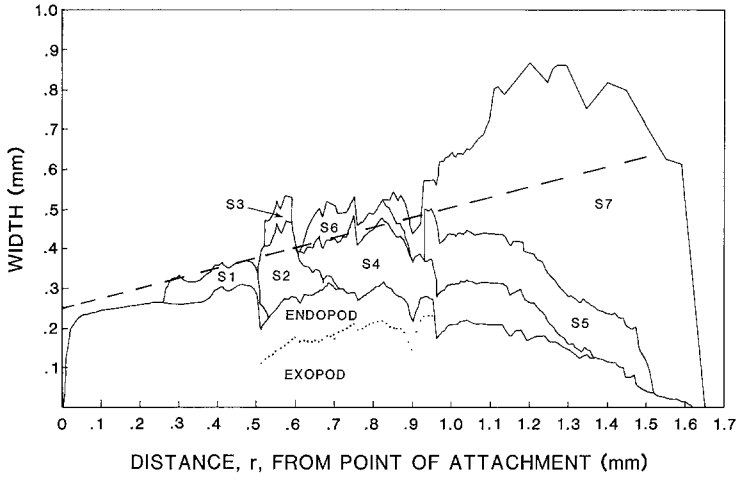

Fig. 5. *Pleuromamma xiphias.* Width of pereiopod shown in Fig. 4 versus radial distance, r, from point of attachment. The different sectors indicate solid portions of setae (S1 through S7) envisioned in a power-stroke orientation. Dashed line is the simplified relationship between width and radial distance used in the model. [Eq. (21) gives the width of a pereiopod pair]

Pereiopod dimensions

The anterior view of the left fourth pereiopod of *Pleuromamma xiphias* is shown in Fig. 4. It was assumed in the model that the exopod and endopod are fully separated and extended, and that the various setae rotate away from the limbs during the power stroke. In this orientation, maximal surface area is exposed. During recovery it is assumed that the large muscles in Basopod 2 pull the exopod in towards the endopod, and the setae (which are inserted posteriorly) rotate passively back and closer to the limbs. Thus, the frontal area is reduced. It also appears that the legs can be folded somewhat closer to the ventral surface of the copepod during recovery by bending posteriorly at several joints.

The setules on the setae are inserted so that they angle posteriorly. The setules probably are able to rotate so as to minimize frontal area during recovery. Because of the boundary layer surrounding each setule, water flow between them will be reduced or absent. Their effectiveness as drag-producing elements depends on their size, spacing, and the Reynolds number of flow. At low values of Re, their effectiveness will increase as boundary layers get thicker. For our model, it was assumed that the setae and setules are as effective as solid blades. The assumption can only overestimate drag and mechanical efficiency of the legs and therefore underestimate swimming cost.

Fig. 5 displays measurements of the width of the single pereiopod (P4) taken from the camera-lucida drawing (Fig. 4) versus distance from pivot point (r). The different sectors indicate different regions of the leg with the setae envisioned in their power-stroke orientation. For the model, the width of the pair of pereiopods (W) was simplified to the function (the dashed line in Fig. 5 represents the width of a single pereiopod, i.e., $W/2$):

$$W_i = 0.33\, l + 0.5\, r_i, \tag{21}$$

where (l) is the total length of the pereiopod (see Table 2 legend for lengths of the legs). The other limbs (P3, P2, P1) were assumed to be geometrically similar.

During recovery it was assumed that only the solid portions (the exopod and endopod) were exposed, and the width was a constant 0.3 mm (0.6 mm for the pair).

Pereiopod movement: power stroke

The force, F_p, acting on the pereiopod was calculated by dividing the leg into 50 cylindrical elements of length Δr_i and width W_i.

The drag ΔD_{ij} [third term in Eq. (1)] on each element is calculated by substituting Eq. (18) for C_d, Eq. (21) for W_i and Eq. (5) for U_i:

$$\Delta D_{ij} = \tfrac{1}{2}\varrho\{1 + 10[\varrho\mu^{-1}(0.5 r_i + 0.33 l) \cdot (\omega_j r_i - V_{Bj}\sin\beta_j)]^{-2/3}\} \cdot (0.5 r_i + 0.33 l)\,\Delta r_i\,(\omega_j r_i - V_{Bj}\sin\beta_j)^2 . \quad (22)$$

The mass (M_i) of each element was assumed to be negligible compared to the added hydrodynamic mass. The mass and added-mass was therefore equal to that of the water contained in the cylindrical volume generated by rotating each paired leg element about its axis multiplied by an added-mass coefficient of 1.0 (Blake, 1979):

$$M_i + \varrho K_I \dot{V}_i = \varrho K_I [(l/6) + (r_i/4)]^2\,\pi\Delta r_i . \quad (23)$$

The force operating on each element (ΔF_{ij}) is, therefore:

$$\Delta F_{ij} = \Delta D_{ij} + \varrho K_I[(l/6) + (r_i/4)]^2\,\pi\,\Delta r_i \cdot \Delta(\omega_j r_i - V_{Bj}\sin\beta_j)(\Delta t_j)^{-1} . \quad (24)$$

The total force, F_p, is the summation of ΔF_{ij} from $i=1$ to 50.

The fluid velocity past each leg section in Eq. (22) was calculated at the midpoint of each time interval (i.e., β and ω were determined from Eqs. (16) and (17) for values of $J=0.5, 1.5, \ldots 49.5$). The acceleration of the fluid past each leg section in Eq. (24) was based on the difference in velocity at the beginning and end of each interval (i.e., for $J=0$ to 1, 1 to 2, ... 49 to 50).

Animal movement: power stroke

The thrust produced by the pereiopods overcomes the parasitic drag of the copepod body and accelerates its mass (M) and hydrodynamic added mass (m).

Substitution of Eq. (20) for added mass, and Eq. (19) for C_d gives:

$$a_j = (\Delta V_{Bj})(\Delta t_j)^{-1} = \{T_j - \tfrac{1}{2}(85.2)(\varrho\, l_c\, V_{B(j-1)}\mu^{-1})^{-0.8}(V_{B(j-1)})^2\varrho A\}(1.12M)^{-1} \quad (25)$$

for the animal body acceleration during interval j.

Recovery stroke

The recovery stroke was analyzed using Eq. (22) except that width was assumed to be a uniform 0.6 mm for the pereiopod pair and the velocity of the legs was constant. Since all the legs move in unison and are assumed to form one packet, the drag of the composite was considered to be equal to that of the largest leg pair, P4. The actual drag will be between the lower limit (drag of just P4) and an upper limit determined by the sum of the drag of four leg pairs moving independently. Because the legs were assumed to be moving at constant velocity, the energy required to accelerate the legs was neglected. Therefore, until further details of leg movements and positions during recovery are revealed in high-speed films, the energy cost of recovery can be stated only as a lower limit.

Coasting

The copepod was assumed to coast with its legs directed forward at 45°. Since it approaches zero velocity asymptotically, a final velocity of 0.001 m s^{-1} (where $Re \sim 1$) was considered as the end of the coasting period. Coasting to still slower speed was considered not justified since the drag coefficients are of uncertain applicability at $Re < 1$.

Animal energetics

Eqs. (8), (9), and (10) were used to calculate the mechanical work performed and the mechanical efficiency of the combined power and recovery strokes. Eq. (11) was used to calculate metabolic work, assuming muscle efficiency is 0.25 (Hill, 1950).

Total cost of transport was based on a respiration rate of 0.5 μl CO_2 $individual^{-1}$ h^{-1} (Morris, unpublished data), an assumed respiratory quotient of 0.8 (mol CO_2:mol O_2), an oxycalorific value of 4.86 kcal l^{-1} O_2 (Gordon, 1977), and the total distance travelled during the swimming episode, i.e., power, recovery and coasting phases.

Active metabolism was determined by dividing the metabolic work (Eq. 11) by the total elapsed time (power plus recovery plus coasting) and adding this to the standard metabolism.

Results

The swimming of *Pleuromamma xiphias* was analyzed at seven different angular pereiopod velocities (identified as Experiments A through G; Table 2) to investigate the relationships between respiration, cost of transport, and mechanical efficiency versus swimming speed. The thrust produced by the pereiopods and the resulting copepod velocity during the power and recovery strokes for the fastest leg rotation (Experiment A) are shown in Fig. 6. The maximal thrust of 2.5×10^{-4} N was produced at $t=3.4$ ms. P4, the first legs to move, were just past their region of maximal drag (normal to the copepod body) and the second set of legs, P3, were accelerating and their added-mass force was large. A similar sudden increase in thrust was caused by the initial movement of P2 and again by P1. The general decrease in thrust produced by successive pereiopods was due in part to the increasing copepod velocity, and, in part, to the progressively smaller dimensions of the legs.

The instantaneous acceleration of the copepod during the power stroke ranged from a maximal value of 53 m s^{-2} at $t=3.4$ ms (when thrust was maximum) to -7 m s^{-2} near the end of the stroke of P1 (thrust was negative because P1

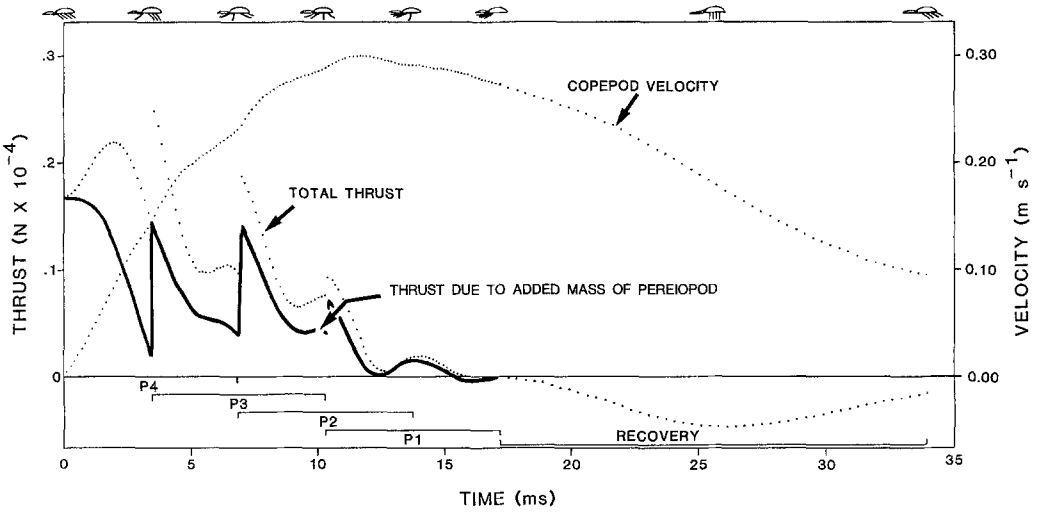

Fig. 6. *Pleuromamma xiphias.* Model prediction for the power and recovery strokes of the fastest leg rotation (Experiment A, see Table 2): time series of copepod velocity and thrust. The portion of the thrust arising from hydrodynamic added-mass is indicated by the lower curve, the remainder arises from drag force. Each point represents a time interval (j) in the computer model

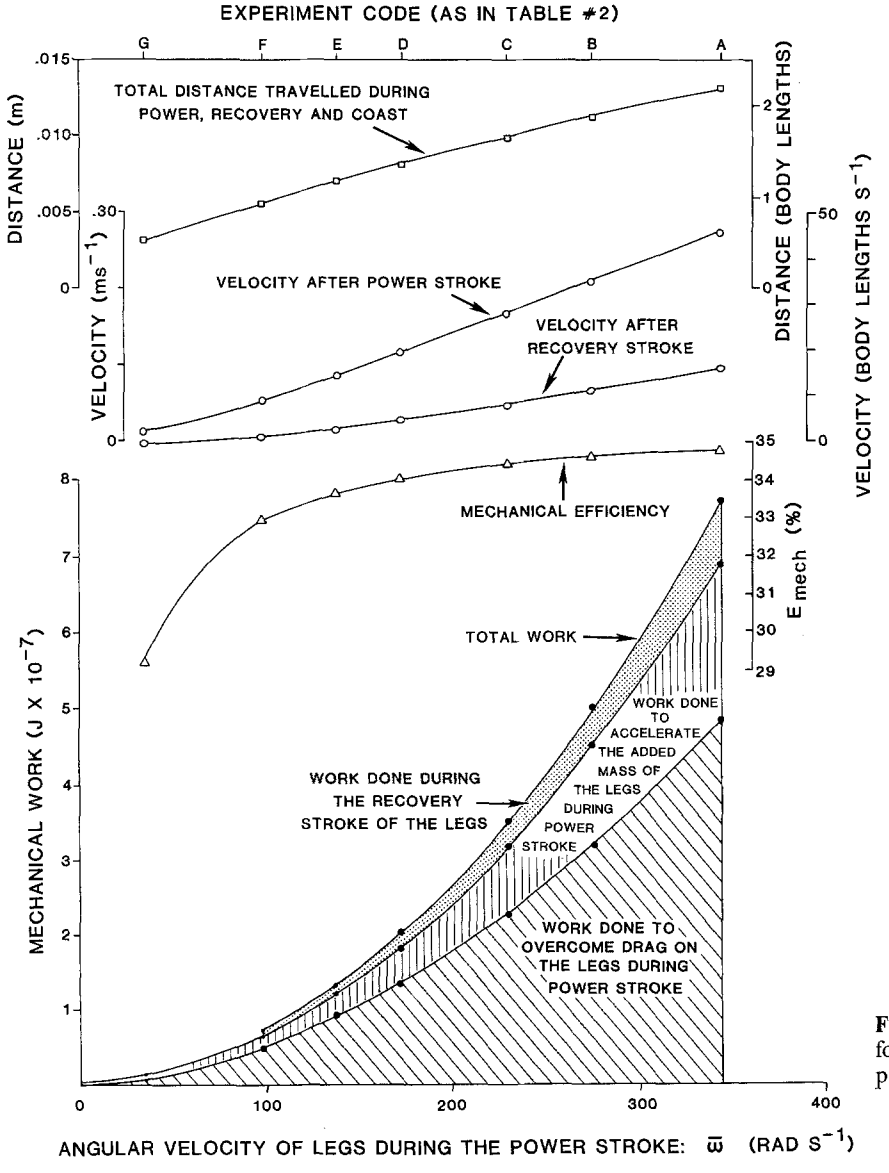

Fig. 7. *Pleuromamma xiphias.* Model predictions for seven angular velocities of the pereiopods (Experiments A through G, see Table 2)

was moving slower than the water flow past the moving copepod).

Maximal copepod velocity, 0.3 m s^{-1}, was reached at $t = 11$ ms or about 70% of the way through the power stroke. The copepod slowed to 0.27 m s^{-1} by the end of the power stroke.

During the recovery phase, a maximal negative thrust of 4.7×10^{-5} N was produced halfway through the stroke (where the legs were normal to the body). The deceleration of the copepod was minimal slightly earlier and was roughly -14 m s^{-2}. The copepod's velocity at the end of the recovery stroke was 0.096 m s^{-1}.

The total work required to move the legs through the power stroke was 6.9×10^{-7} J. Of this, roughly 30% was used for accelerating the added mass of the pereiopods; the remainder was required to overcome their drag.

During the initial stages of each pereiopod's power stroke, the copepod did work to accelerate the added mass of the leg. The force exerted produced thrust. In the latter half of the stroke the leg was decelerating and the added-mass force was negative. During this period, the added-mass force opposed the drag force, decreasing the thrust. In angelfish, the added-mass force during deceleration exceeded the drag force (Blake, 1979). Consequently, the fish had to do work to decelerate its fins in addition to accelerating them in the power stroke. In our model, the added-mass force of the legs during deceleration was less than their opposing drag force except during the latter third of the stroke of the smallest legs, P1 (Fig. 6). Therefore, the force required to slow down the legs was supplied by their drag, that is, the legs coasted through the later stages of their stroke. The copepod did not work to decelerate its legs, but it did suffer a loss of thrust.

The results of the power strokes at other speeds are summarized in Table 2 and shown in Fig. 7. Copepod velocities ranged from 0.27 m s^{-1} for the fastest leg rotation (Experiment A) to 0.01 m s^{-1} for the slowest (Experiment G). Average accelerations ranged from 15.97 m s^{-2} for A to 0.07 m s^{-2} for G. Thus, a 10-fold increase in pereiopod angular velocity produced a 27-fold increase in final copepod velocity and a 230-fold increase in average acceleration. The fastest stroke (Experiment A) required 70 times more work than the slowest. The distance travelled by the copepod during the power stroke varied only a little, from 3.80×10^{-3} m (A) to 2.71×10^{-3} m (G).

The work done in returning the legs to their original positions ranged from 8.12×10^{-8} to 0.07×10^{-8} J for Experiments A and G, respectively (Table 3, Fig. 7). The copepod continued to move in the forward direction but slowed during the recovery stroke. The distance travelled ranged from 3.16×10^{-3} m (A) to 0.47×10^{-3} m (G). The

Table 2. *Pleuromamma xiphias.* Results of analysis of power-stroke sequence. Model parameters are pereiopod lengths (1.5, 1.4, 1.35, and 1.0 mm for P4, P3, P2, P1, respectively), copepod dimensions (4 mg mass, 6 mm length, and 3.14×10^{-6} m^2 frontal area), seawater density (1 024 kg m^{-3}), temperature (20 °C), and dynamic viscosity (1.072×10^{-3} kg m^{-1} s^{-1}). The adjustable parameter is mean pereiopod angular velocity, (A) – (G)

Angular velocity [mean (max.) rad s^{-1}]	Work done in moving legs ($J \times 10^{-7}$)	Final velocity (m s^{-1})	Distance travelled ($m \times 10^{-3}$)	Average acceleration (m s^{-2})
(A) 343 (539)	6.92	0.27	3.80	15.97
(B) 274 (431)	4.50	0.21	3.74	9.81
(C) 229 (359)	3.18	0.17	3.69	6.56
(D) 172 (270)	1.85	0.12	3.58	3.44
(E) 138 (216)	1.21	0.09	3.49	2.06
(F) 98 (154)	0.65	0.06	3.33	0.93
(G) 34 (53.9)	0.10	0.01	2.71	0.07

Table 3. *Pleuromamma xiphias.* Results of recovery stroke. Pereiopod velocity was 2.5 times lower than the mean velocity in the power stroke. During recovery the copepod continued to move forward (distance travelled), but slowed down to the final velocity indicated

Work done in moving legs ($J \times 10^{-8}$)	Distance travelled ($m \times 10^{-3}$)	Final velocity (m s^{-1})	Mechanical efficiency (%)
A 8.12	3.16	0.096	34.8
B 5.04	2.93	0.066	34.6
C 3.41	2.72	0.048	34.4
D 1.83	2.38	0.027	34.0
E 1.13	2.09	0.017	33.6
F 0.55	1.66	0.006	32.9
G 0.07	0.47	−0.003	29.2

Table 4. *Pleuromamma xiphias.* Results of coasting and summary of entire swimming episode. Net cost of transport was calculated by assuming that muscle efficiency in copepods is 25%

Distance travelled during coasting ($m \times 10^{-3}$)	Total distance travelled ($m \times 10^{-3}$)	Total work done ($J \times 10^{-7}$)	Average velocity during episode swimming		Active:routine metabolism	Net cost of transport (cal g^{-1} km^{-1})
			(m s^{-1})	(body lengths s^{-1})		
A 6.17	13.13	7.73	0.032	5.2	3.1	14.1
B 4.56	11.23	5.01	0.028	4.6	2.4	10.7
C 3.49	9.90	3.52	0.025	4.2	2.0	8.5
D 2.17	8.13	2.03	0.022	3.6	1.6	6.0
E 1.40	6.99	1.33	0.019	3.2	1.4	4.5
F 0.57	5.57	0.71	0.018	2.9	1.3	3.0
G 0	3.17	0.11	0.009	1.5	1.0	0.8

copepod velocity at the end of the recovery stroke (Fig. 7) ranged from 0.096 m s^{-1} (A) to a slight negative velocity, −0.003 m s^{-1} for G.

The distance travelled during the coasting period and the cumulative distance for the entire episode are presented in Table 4. The total distance ranged from 13.13×10^{-3} m (2.2 body lengths) for the fastest to 3.17×10^{-3} m (0.5 body lengths) for the slowest (Table 4). The average velocity during the episode was 0.032 m s^{-1} for Experiment A and 0.009 m s^{-1} for G. Expressed as body lengths per second, these are 5.2 and 1.5, respectively. Thus, a 10-fold increase in leg angular velocity resulted in only a 3.5-fold increase in average swimming velocity.

Discussion

The model predicts several quantities that may be compared to published observations. Both the pattern of body velocity with time and the maximal velocity attained by Stage V copepodites of the calanoid *Calanus helgolandicus* (3.0 mm cephalothorax length) swimming in a hopping mode (Petipa, 1981) are in close agreement with our model results. *C. helgolandicus* reached a maximal velocity of 0.28 m s^{-1} compared to our model prediction of 0.30 m s^{-1} for *Pleuromamma xiphias*. Maximal velocity for both species was reached during the stroke of the second pereiopod (see Fig. 63 of Petipa, 1981; and present Fig. 6).

Maximal swimming velocities have been reported for three other copepod species: *Labidocera trispinosa:* 0.10 m s^{-1} (1.0 mm cephalothorax length, Calanoida; Vlymen, 1970); *Cyclops securifer:* 0.25 m s^{-1} (0.5 mm, Cyclopoida; Strickler and Bal, 1973); and *Diaptomus franciscanus:* 0.20 m s^{-1} (1.5 mm, Calanoida; Lehman, 1977). Our value of 0.30 m s^{-1} for the maximal swimming velocity of *Pleuromamma xiphias* is slightly higher than the reported range. This is not surprising, since *P. xiphias* is approximately four times the size of the largest copepod (*D. franciscanus:* 1.5 mm vs *P. xiphias:* 6.0 mm) and maximal swimming velocity scales with body length (Beamish, 1978).

Average acceleration of *Pleuromamma xiphias* during the power stroke sequence in Experiment A was 16 m s^{-2}, quite similar to Strickler's (1975) observed average acceleration for *Cyclops* sp. of 12 m s^{-2}. In contrast, our model prediction for maximum instantaneous acceleration (53 m s^{-2}) was more than three times higher than that for average acceleration. However, the time intervals of the model are equivalent to a filming rate of 7 000 frames s^{-1}, which is more than ten times faster than has been used in any reported cinematic study.

The mechanical efficiency (E_{mech}) of the propulsion system of *Pleuromamma xiphias* showed a slight increase with increasing swimming speed and was between 0.30 and 0.35 except for the slowest movement (Experiment G). The corresponding swimming efficiency (E_{aer}) is approximately 0.08 if muscle efficiency is assumed to be 0.25 (Hill, 1950). A similar pattern of increased efficiency with increased swimming speed has been reported for two other species that use paddle propulsion. The green turtle *Chelonia myadas* (Prange, 1976) had swimming efficiencies similar to *P. xiphias* (E_{aer}=0.01 to 0.10). The euphausiid *Euphausia pacifica* (Torres, 1984) had lower swimming efficiencies (E_{aer}=0.001 to 0.028). Angelfish, which swim by pectoral fin propulsion, were also less efficient. Their mechanical efficiency was about one-half that of *P. xiphias* (E_{mech}=0.16; Blake, 1980). These values are in contrast to the high mechanical efficiency (E_{mech}=0.75) of fusiform fish swimming in the undulatory mode (Lighthill, 1970).

The most important model prediction is the energy expended by the copepod while swimming. Published estimates of crustacean locomotory costs fall into two groups:

Group 1: calculated values for small animals that indicate low cost of swimming (Vlymen, 1970; Klyashtorin and Yarzhombek, 1973; Svetlichnyi *et al.*, 1977);

Group 2: empirical determinations for larger crustaceans that indicate high swimming costs (e.g. Ivlev, 1963; Torres and Childress, 1983).

Our model predicts a ratio of active to standard metabolism (metabolic scope; Fry, 1971) of more than 3 at maximum swimming speed (Fig. 8). This is similar to the empirically determined values of metabolic scope in larger crustaceans (2.5 to 3.0 for Group 2 above), and is much larger than the calculated values (1.01 to 1.25 for Group 1 above).

Our model differs from previous calculations of copepod swimming energetics in that: (1) the mechanical efficiency of the propulsion system was determined including the energy loss of the recovery strokes; (2) the

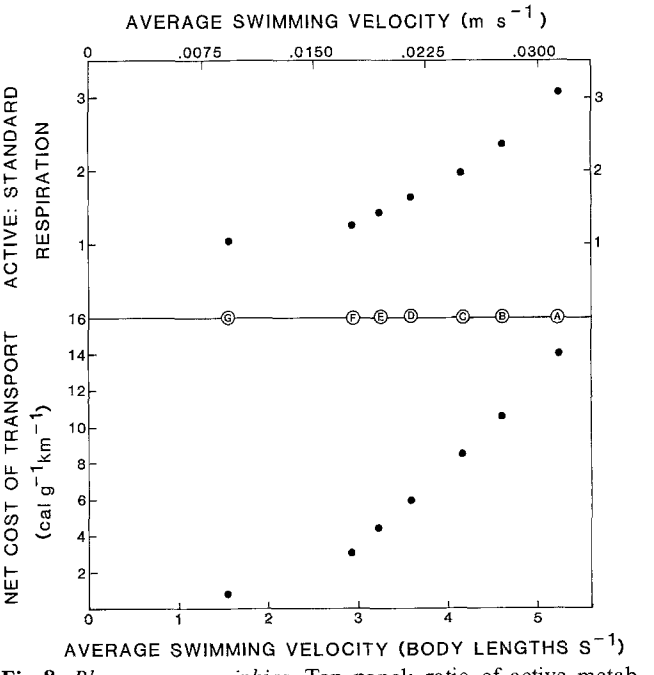

Fig. 8. *Pleuromamma xiphias.* Top panel: ratio of active metabolism to standard metabolism (metabolism at rest) at different swimming velocities. Bottom panel: Net cost of transport versus average swimming speed

effects of hydrodynamic added-mass were calculated for the accelerating pereiopods as well as the copepod body; (3) swimming costs were based on intermittent, non-steady motion.

Klyashtorin and Yarzhombek (1973) used the mechanical efficiency of a paddle wheel operating at high Reynolds number ($E_{mech}=0.50$) to calculate swimming cost in copepods. This value was also used by Svetlichnyi *et al.* (1977), while Vlymen (1970) assumed $E_{mech}=1.0$. In contrast, our model indicates a lower value for E_{mech}. The overall efficiency of the fastest leg rotation (Experiment A) was 0.34, about 10% lower than the efficiency of the power stroke alone ($E_{mech}=0.38$). This 10% decrease is similar to the pattern in angelfish, where an 11% decrease in E_{mech} was shown for the inclusion of recovery stroke (Blake, 1980). If our predicted value of E_{mech} is correct, copepod swimming costs were underestimated by factors of 3 and 1.5, respectively, by Vlymen (1970) and Klyashtorin and Yarzhombek (1973).

Although the hydrodynamic added-mass of copepod bodies has usually been included in calculations of swimming costs (e.g. Vlymen, 1970), the added mass of the swimming appendages has not. The relative importance of the effect is suggested by comparing the maximal acceleration of the copepod to the maximal acceleration of its pereiopods. In Experiment A, maximal body acceleration was 53 m s^{-2}, whereas the tangential acceleration at the tip of P4 reached 370 m s^{-2}. Out model indicates that for *Pleuromamma xiphias,* 20 to 30% of the mechanical energy required to swim is used to accelerate the added mass of its pereiopods. The effect of hydrodynamic added-mass is that of increasing the swimming efficiency of *P. xiphias.* When the model was modified by changing the added-mass coefficient, K_I, of the pereiopod, [see Eq. (2)] from 1.0 to 0.3 and then to zero, the mechanical efficiency dropped from 0.34 to 0.20 and to 0.15, respectively.

Our model indicates that large errors can arise if swimming energy is based on an averaged velocity rather than the true unsteady-velocity time-history. For example, in Experiment A, the mean velocity during the swimming episode was 0.031 m s^{-1}. The rate of mechanical energy dissipation through body drag for *Pleuromamma xiphias* moving at this constant velocity would be 6.7×10^{-8} W. However, the power dissipated as drag when the individual moves at the variable velocities predicted by the model was 7×10^{-7} W, or roughly an order of magnitude higher. The drag increase due to non-steady swimming has also been demonstrated by Minkina and Pavlova (1981) for a calanoid copepod of similar size. *Calanus helgolandicus* (mean speed 2 cm s^{-1}) expended metabolic power at the rate of 15.3×10^{-4} cal h^{-1} in a variable swimming regime, which was two orders higher than for constant velocity swimming at the same speed. The model prediction for *P. xiphias* swimming at a similar average velocity (Experiment E) was very similar at 12.7×10^{-4} cal h^{-1}.

A comparison of net cost of transport (Fig. 9) is an excellent means of examining the swimming costs of *Pleuromamma xiphias* relative to other swimmers of different sizes and propulsive techniques (cf. Tucker, 1970; Schmidt-Nielsen, 1972; Beamish, 1978; Torres, 1984). Cost of transport was calculated from the oxygen available for propulsion at 75% of a species' critical swimming speed (U_{crit}) from the literature cited in the legend to Fig. 9. 75% U_{crit} approximates the swimming velocity at which peak muscular efficiency occurs (Webb, 1971) and is easily compared with previous literature on cost of transport (Tucker, 1970; Schmidt-Nielsen, 1972; Beamish, 1978).

Net cost of transport for *Pleuromamma xiphias* was based on 75% of maximal velocity and was estimated by taking copepod velocity at the end of Power Stroke A (0.27 m s^{-1}) as an upper limit, and that of Power Stroke B (0.21 m s^{-1}) as a lower limit. The corresponding costs of transport were 10 cal g^{-1} km^{-1} and 7.6 cal g^{-1} km^{-1}, respectively.

The continuous line in Fig. 9 represents a regression of net cost of transport vs weight for the sockeye salmon *Oncorhynchus nerka* (Brett and Glass, 1973). If the regression is extrapolated to the size range of copepods (dashed line), a cost of transport of 5.6 cal g^{-1} km^{-1} is predicted for *Pleuromamma xiphias.* Values predicted by the model are 1.4 to 1.8 times higher than that for *O. nerka,* but lower than values determined for other crustaceans (these are 3 times to 5 times higher than the salmon values). Our model prediction falls between the lower limit based on highly-efficient fish propulsion and the upper limit of low-efficiency multiple-paddle propulsion of euphausiids and decapods. The predicted efficiency for *P. xiphias* is intermediate to these two groups of swimmers.

The model is based on several simplifying assumptions. The blade-element approach (Blake, 1979, 1980) used here treats the flow pattern around the pereiopod as a series of two-dimensional flows. Variation of shape along the length of the leg, flow between setules, and flow around the free ends of the leg and setae have been considered second-order effects and thus were omitted.

The influence of the boundary layer near the animal body and the effect of the wakes of adjacent swimming appendages have also been omitted. However, the close agreement between published values of swimming velocities and the model predictions for *Pleuromamma xiphias* suggest that these effects may be unimportant in copepod locomotion. Boundary-layer influence is minimal because most of the thrust generated by the pereiopods is produced by the distal segments which have greater area and are moving faster than those located close to the copepod's body. Flow interaction between legs is minimized by the stroke pattern of the legs. During the power phase, only two legs are moving at most and the posterior to anterior pattern moves the copepod into undisturbed fluid before each leg begins its stroke. It is expected that flow interactions between pleopods may be important to crustaceans that display other patterns of swimming strokes. For example, the pleopods of euphausiids move metachronally from posterior to anterior. The last leg to move, Pleopod 1, ends its power stroke as Pleopod 5 finishes its recovery

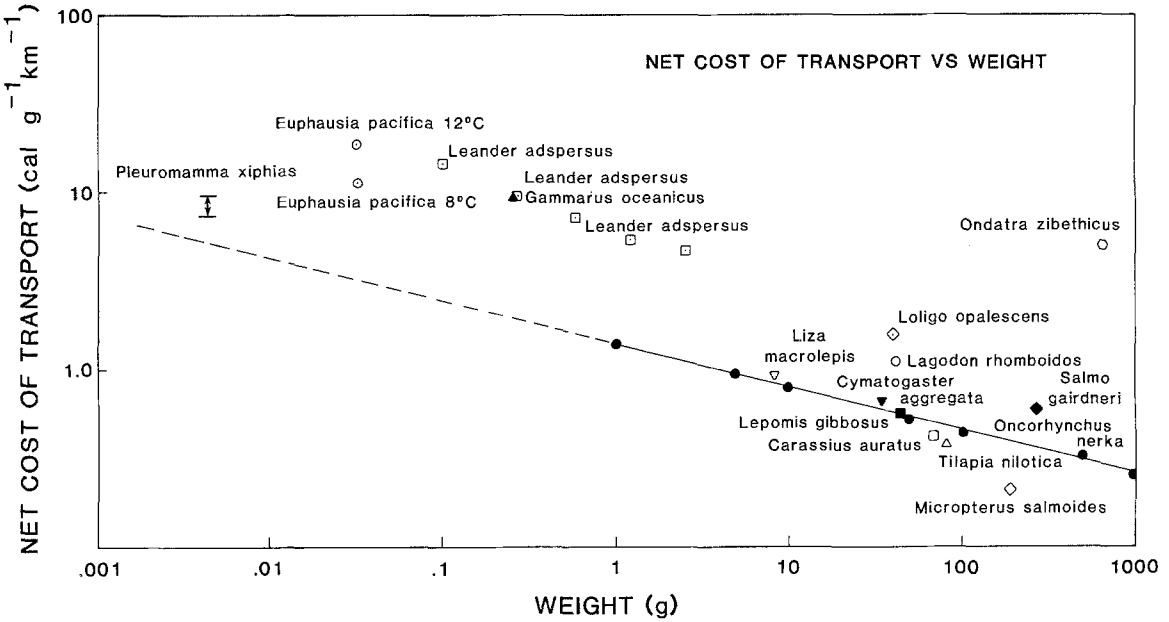

Fig. 9. Net cost of transport as a function of weight for 13 swimming species (after Schmidt-Nielsen, 1972; Beamish, 1978). Cost was calculated at 75% of critical swimming speed if data were available. If not, averaged swimming speed was used. Temperature chosen for calculation was 15 °C or that closest to 15 °C. Values for the copepod *Pleuromamma xiphias* were calculated at 75% of velocity after power stroke (Experiments A and B, Table 2). Continuous line represents a regression of cost of transport vs weight for *Oncorhynchus nerka* between 1 and 1 000 g, from data in Brett and Glass [1973; equation: $y = 1.416\ w^{-0.25}$, y = net cost of transport (cal g^{-1}), w = weight (g), $r = 0.99$]; dashed line is an extrapolation of the continuous line into weight values typical of zooplankton species, for purposes of comparison. Data from the following papers were used to construct this graph: *Carassius auratus*: Smit *et al.* (1971); *Cymatogaster aggregata:* Webb (1975); *Euphausia pacifica:* Torres and Childress (1983); *Gammarus oceanicus:* Halcrow and Boyd (1967); *Lagodon rhomboides*: Wohlschlag *et al.* (1968); *Lepomis gibbosus:* Brett and Sutherland (1965) *Liza macrolepis:* Kutty (1969); *Loligo opalescens:* O'Dor (1982); *Micropterus salmoides:* Beamish (1970); *Salmo gairdneri:* Webb (1971); *Tilapia nilotica:* Farmer and Beamish (1969); *Leander adspersus:* Ivlev (1963); *Ondatra zibethicus:* Fish (1982)

stroke (Kils, 1981). Thus, for the euphausiids, Pleopod 5 must move forward through fluid that has been accelerated by the other appendages, and modeling their propulsion requires the incorporation of an interaction term.

Additionally, the variation of added-mass coefficient with Reynolds number and of added-mass coefficient and drag coefficient with leg-period parameter was considered negligible. The simplifying assumptions were made primarily because of lack of data rather than computational complexities, and can be corrected in the model as quantitative information becomes available.

Only forces operating in line with the rectilinear motion of the copepod have been considered. A complete analysis of forces includes gravity, buoyancy, and the pitch and yaw components of hydrodynamic force. These may also be later incorporated in the model and will provide an additional prediction with which the model can be tested, specifically the trajectory and time course of body attitudes.

Due to the general lack of data concerning copepod swimming, our application of the model to *Pleuromamma xiphias* was based on assumptions about its swimming behavior, i.e., the positions and velocities of the swimming appendages over time, which limbs are involved, and the pattern of behavior (the timing of power, recovery, and coasting phases). The cumulative error arising from these assumptions and from the simplifications in theory may be quantified by comparing the velocity and acceleration of the animal predicted from the model with observed velocities and accelerations in future high-speed films of swimming animals.

Despite the assumptions that were necessary in formulating the model, the biomechanical parameters (maximal velocity, average acceleration, mechanical efficiency) are within the expected range of values dictated by published observations. Model predictions of energetic parameters (cost of transport, swimming efficiency, and metabolic scope) are in excellent agreement with the experimental observations on larger crustaceans in the literature. Thus, our model narrows the disparity between the theoretical and empirical data bases.

The model is both experimentally verifiable and flexible. It is applicable to the movement of any crustacean limb, and can thus be used to analyze feeding as well as locomotion with minor modification. Use of our model and future models of this type should allow for cost-benefit analyses of all aspects of crustacean behavior that can be recorded on film.

Acknowledgements. The authors would like to thank Ms. C. Cunningham and Miss D. Bombard for typing the manuscript, Ms. D. Walton for preparing the graphics and Mr. P. McGillibary and Ms. G. Gust for translations of Russian works. The first author was supported by a fellowship from the Gulf Oceanographic Charitable Trust. Although not specifically cited, S. Vogel's book entitled "Life in moving fluids" was inspirational.

Literature cited

Beamish, F. W. H.: Oxygen consumption of largemouth bass *Micropterus salmoides,* in relation to swimming speed and temperature. Can. J. Zool. *48,* 1221–1228 (1970)

Beamish, F. W. H.: Swimming capacity. *In:* Fish physiology, Vol. 7. pp 101–187. Ed. by W. S. Hoar and D. J. Randall. London and New York: Academic Press 1978

Blake, R. W.: The mechanics of labriform locomotion. I. Labriform locomotion in the angelfish (*Pterophyllum cimekei*): an analysis of the power stroke. J. exp. Biol. *82,* 255–271 (1979)

Blake, R. W.: The mechanics of labriform locomotion. II. An analysis of the recovery stroke and the overall fin beat cycle propulsive efficiency in the angelfish. J. exp. Biol. *85,* 337–342 (1980)

Brett, J. R. and N. R. Glass: Metabolic rates and critical swimming speeds of sockeye salmon (*Oncorhynchus nerka*) in relation to size and temperature. J. Fish. Res. Bd Can. *30,* 379–387 (1973)

Brett, J. R. and D. B. Sutherland: Respiratory metabolism of pumpkinseed (*Lepomis gibbosus*) in relation to swimming speed. J. Fish. Res. Bd Can. *22,* 405–409 (1965)

Farmer, G. J. and F. W. H. Beamish: Oxygen consumption of *Tilapia nilotica* in relation to swimming speed and salinity. J. Fish. Res. Bd Can. *26,* 2807–2821 (1969)

Fish, F. E.: Aerobic energetics of surface swimming in the muskrat *Ondatra zibethicus.* Physiol. Zoöl. *55,* 180–189 (1982)

Fry, F. E. J.: The effect of environmental factors on the physiology of fish. *In:* Fish physiology, Vol. 6. pp 1–98. Ed. by W. S. Hoar and D. J. Randall, London and New York: Academic Press 1971

Gordon, M. S.: Animal physiology: principles and adaptations, 592 pp. New York: Macmillan 1977

Goring, D. G. and F. Raichlen: Forces on block bodies accelerating in still fluid. J. Am. Soc. civil Engrs (Waterway, Port, cstl Ocean Div.) *105 (WW2),* 171–189 (1979)

Halcrow, K. and C. M. Boyd: The oxygen consumption and swimming activity of the amphipod *Gammarus oceanicus* at different temperatures. Comp. Biochem. Physiol. *23,* 233–242 (1967)

Hill, A. V.: The dimensions of animals and their muscular dynamics. Sci. Prog., Lond. *38,* 209–230 (1950)

Hoerner, S. F.: Fluid-dynamic drag, S. F. Hoerner, 2 King Lane, Greenbriar, Bricktown, N.J. 08723, USA (1965)

Hopkins, T. L.: The vertical distribution of zooplankton in the Eastern Gulf of Mexico. Deep-Sea Res. *29,* 1069–1083 (1982)

Ivlev, V. S.: Energy consumption during the motion of shrimps. Zool. Zh. *42,* 1465–1471 (1963)

Kils, U.: The swimming behavior, swimming performance and energy balance of antarctic krill, *Euphausia superba.* BIOMASS scient. Ser. *3,* 1–121 (1981)

Klyashtorin, L. B. and A. A. Yarzhombek: Energy consumption in movement of planktonic organisms. Oceanology *13,* 575–580 (1973)

Kutty, M. N.: Oxygen consumption in the mullet *Liza macrolepis* with special reference to swimming velocity. Mar Biol. *4,* 239–242 (1969)

Lehman, J. T.: On calculating drag characteristics for decelerating zooplankton. Limnol. Oceanogr. *22,* 170–172 (1977)

Lighthill, M. J.: Aquatic animal propulsion of high hydrodynamic efficiency. J. Fluid Mech. *44,* 265–301 (1970)

Lighthill, M. J.: Aquatic animal propulsion. Int. Congr. appl. Mech. (Moscow) *13,* 29–46 (1972)

Minkina, N. I. and E. V. Pavlova: Hydrodynamic drag and power at variable swimming in *Calanus helgolandicus* (Claus). Ekol. Morila *7,* 63–75 (1981)

Morrison, J. R., M. P. O'Brien, J. W. Johnson and S. A. Schaat: The forces exerted by surface waves on piles. J. Petrol. Technol. *189 (TP2846),* 149–189 (1950)

Nachtigall, W.: Locomotion mechanics and hydrodynamics of swimming in aquatic insects. *In:* The physiology of insects, Vol. 3. pp 381–432. Ed. by M. Rockstein. New York: Academic Press 1974

Nachtigall, W.: Swimming mechanics and energetics of locomotion of variously sized water beetles – Dytiscidae, body lengths 2 to 35 mm. *In:* Scale effects in animal locomotion, pp 269–283. Ed. by T. J. Pedley. London: Academic Press 1977

O'Dor, R. K.: Respiratory metabolism and swimming performance of the squid, *Loligo opalescens.* Can. J. Fish. aquat. Sciences *39,* 580–587 (1982)

Petipa, T. S.: Trophic dynamics of copepods in marine planktonic systems, 245 pp. [In Russ.]. Kiev: Naukowa Dumka 1981

Prange, H. D.: Energetics of swimming of a sea turtle. J. exp. Biol. *64,* 1–12 (1976)

Quetin, L. B., T. J. Mickel and J. J. Childress: A method for simultaneously measuring the oxygen consumption and activity of pelagic crustaceans. Comp. Biochem. Physiol. *59A,* 263–266 (1978)

Schmidt-Nielsen, K.: Locomotion: energy cost of swimming, flying, and running. Science, N.Y. *177,* 222–228 (1972)

Smit, H., J. M. Amelink-Koutstall, J. Vijverberg, and J. C. von Vaupel-Klein: Oxygen consumption and efficiency of swimming goldfish. Comp. Biochem. Physiol. *39A,* 1–28 (1971)

Strickler, J. R.: Swimming of planktonic *Cyclops* species (Copepoda, Crustacea): pattern, movements, and their control. *In:* Swimming and flying in nature, Vol. 2. pp 599–613. Ed. by T. Y. T. Wu, C. J. Brokaw and C. Brennan. New York: Plenum Press 1975

Strickler, J. R. and A. K. Bal: Setae on the first antennae of the copepod *Cyclops scutifer* (Sars): their structure and importance. Proc. natn. Acad. Sci. U.S.A. *70,* 2656–2659 (1973)

Svetlichnyi, L. S., Yu. A. Zagorodnyaya and V. N. Stepanov: Bioenergetics of copepods *Pseudocalanus elongatus* during migration. Soviet J mar. Biol. *3,* 430–436 (1977)

Thom, A. and P. Swart: The forces on an aerofoil at very low speeds. Jl R. aeronaut. Soc. *44,* 761–770 (1940)

Torres, J. J.: Relationship of oxygen consumption to swimming speed in *Euphausia pacifica.* II. Drag, efficiency and a comparison with other swimming organisms. Mar. Biol. *78,* 231–237 (1984)

Torres, J. J. and J. J. Childress: Relationship of oxygen consumption to swimming speed in *Euphausia pacifica.* 1. Effects of temperature and pressure. Mar. Biol. *74,* 79–86 (1983)

Torres, J. J., J. J. Childress and L. B. Quetin: A pressure vessel for the simultaneous determination of oxygen consumption and swimming speed in zooplankton. Deep-Sea Res. *29,* 631–639 (1982)

Tucker, V. A.: Energetic cost of locomotion in animals. Comp. Biochem. Physiol. *34,* 841–846 (1970)

Vlymen, W. J.: Energy expenditure of swimming copepods. Limnol. Oceanogr. *15,* 348–356 (1970)

Webb, P. W.: The swimming energetics of trout. (I) Oxygen consumption and swimming efficiency. J. exp. Biol. *55,* 521–540 (1971)

Webb, P. W.: Efficiency of pectoral-fin propulsion of *Cymatogaster aggregata. In:* Swimming and flying in nature, pp 573–584. Ed. by T. Y. T. Wu, C. J. Brokaw and C. Brennen. New York: Plenum Press 1975

White, F. M.: Viscous fluid flow, 640 pp. New York: McGraw-Hill 1974

Wohlschlag, D. E., J. N. Cameron and J. J. Cech, Jr.: Seasonal changes in the respiratory metabolism of the pinfish (*Lagodon rhomboides*). Contr. mar. Sci. Univ. Tex. *13,* 89–104 (1968)

Date of final manuscript acceptance: February 26, 1985.
Communicated by J. M. Lawrence, Tampa